Am J Transl Res 2023;15(6):3960-3975
www.ajtr.org /ISSN:1943-8141/AJTR0147081

Original Article

The expression panel of CXCL9, GBP5, and IFNG is a potential pan-cancer biomarker to predict immunotherapy response

Jingpu Wang[1,2], Yuan Zhou[3], Yang Yang[4], Zhouqiao Wu[2]

[1]Department of Surgery, University Medical Center Utrecht, Utrecht, The Netherlands; [2]Key Laboratory of Carcinogenesis and Translational Research (Ministry of Education), Department of Gastrointestinal Surgery, Peking University Cancer Hospital and Institute, Beijing, China; [3]Department of Biomedical Informatics, School of Basic Medical Sciences, Peking University, Beijing, China; [4]Department of Thoracic Surgery, The First Affiliated Hospital, Zhengzhou University, Zhengzhou, Henan, China

Received October 18, 2022; Accepted February 7, 2023; Epub June 15, 2023; Published June 30, 2023

Abstract: Background: The effectiveness of immunotherapy has been validated in multiple cancers. However, not all patients benefit from immunotherapy, and its objective response rate is less than 30% in some cancers, so it is of great importance to find a pan-cancer biomarker that can effectively predict immunotherapy response. Methods: Fifteen immunotherapy datasets were retrospectively analyzed to determine pan-cancer biomarkers to predict immunotherapy response. A total of 348 patients with metastatic urothelial carcinoma (mUC) who received anti-PD-L1 immunotherapy from the dataset of IMvigor210 trial were included in the primary analysis. In addition, 12 public immunotherapy datasets of different cancers and two datasets of gastrointestinal cancer patients who received anti-PD-1 or anti-PD-L1 immunotherapy between August 2015 and May 2019 at Peking University Cancer Hospital (PUCH) were analyzed as validation cohorts. Results: The expression of CXCL9, IFNG, and GBP5 was independently associated with the response to anti-PD-L1 immunotherapy in patients with mUC. The ability of the expression panel of CXCL9, IFNG, and GBP5 to predict immunotherapy response was validated in immunotherapy datasets of different cancers. Conclusion: The expression panel of CXCL9, IFNG, and GBP5 can potentially be a pan-cancer biomarker for predicting immunotherapy response.

Keywords: Immunotherapy, pan-cancer, biomarker

Introduction

In the past decade, the introduction of immune checkpoint inhibitors (ICIs) has dramatically influenced the oncology care landscape. The efficacy of ICIs has now been demonstrated in several cancers, including melanoma, non-small cell lung cancer, urinary system cancer, gastric cancer, etc. [1-4]. However, not all cancer patients can benefit from ICIs, and their objective response rate is even less than 30% for some cancers [5, 6]. Patients who do not respond to ICIs may not only fail to obtain a significant survival benefit but may even suffer from the adverse events of ICIs [7-9]. Therefore, finding effective biomarkers to predict the response to immunotherapy is crucial to identify immunotherapy target populations and improve treatment strategies for cancer patients. Several indicators have been suggested to have potential as biomarkers, including PD-L1, tumor-infiltrating lymphocytes, tumor mutational burden (TMB), tumor neoantigen burden (TNB), and INF-γ [10]. In addition to the potential biomarkers above, little is known about whether other genes are differentially expressed between tumor tissues of responders and nonresponders to immunotherapy, and this information may improve the current prediction strategies. This study aims to use data with a large sample size from a phase II trial of atezolizumab in metastatic urothelial cancer (mUC) to identify potential predictive biomarkers of immunotherapy response. In addition, validation cohorts of patients with different cancers receiving different immunotherapies,

including two datasets from Peking University Cancer Hospital (PUCH) and public datasets, were used to validate their potential for pan-cancer applications.

Materials and methods

Data collection

Fifteen immunotherapy datasets were retrospectively analyzed to identify pan-cancer biomarkers for predicting immunotherapy response. The transcriptome profiles of the preimmunotherapy tumor samples of 348 patients with mUC treated with atezolizumab from the IMvigor210 study were used to screen potential biomarkers [11]. The study cohorts of Alexandra et al., Braun et al., Chen et al., Gide et al., Hugo et al., Lauss et al., Nathanson et al., Prat et al., Kim et al. and Riaz et al. were included as external validation cohorts to validate the predictive ability of the biomarkers [12-21]. In addition, 75 gastrointestinal cancer patients who received anti-PD-1 or anti-PD-L1 immunotherapy between August 2015 and May 2019 at our center (PUCH), and had pretreatment tumor tissue transcriptome profiles as well as information on the level of response to immunotherapy, were also included in this study as validation datasets. The transcriptome profiles of 33 cancers from The Cancer Genome Atlas (TCGA) database (https://portal.gdc.cancer.gov/) were used to perform the pan-cancer analysis.

Identification of differentially expressed genes (DEGs)

Because the accuracy of assessing patients' immunotherapy response clinically is affected by several factors, the response levels of some patients may be incorrectly divided into adjacent response level categories. For a more accurate identification of genes that can influence the immunotherapy response, we only compared patients with progressive disease (PD) and those with complete response (CR) to identify DEGs. The "limma" package of R software was used to determine the DEGs between PD and CR patients, and genes with adjusted $P < 0.05$ were considered DEGs.

GO term and KEGG pathway enrichment analyses

To explore the biological significance of the DEGs, we used the "clusterProfiler" package of R software for functional and pathway enrichment analyses of DEGs. $P < 0.05$ was considered significant enrichment.

Screening of genes associated with immunotherapy response and establishment of CIG score

Search Tool for the Retrieval of Interacting Genes (STRING, Zurich, Switzerland, https://string-db.org/), which contains relevant information on functional and physical associations between proteins, was used to construct protein-protein interaction (PPI) networks in this study. Confidence values > 0.4 were defined as significant associations. The PPI results were imported into Cytoscape software for PPI network analysis. The maximal clique centrality (MCC) algorithm is an effective way to find the central nodes in a PPI network. The cytoHubba tool in Cytoscape software was used to calculate the MCC value of each node, and the genes whose MCC value ranked in the top 10 were considered as the hub genes [22]. The hub genes and the DEGs with |log2 fold change (log2 FC)| > 1 were included in multivariate logistic regression, and genes with P value < 0.05 were considered predictive genes. Patients with CR and partial response (PR) were considered responsive to immunotherapy, and patients with stable disease (SD) and PD were considered unresponsive to immunotherapy. The predictive genes were included in multivariable logistic regression to calculate the regression coefficient (coef), and a CIG score for each patient was calculated based on the predictive gene expression and the coef as follows:

$$\text{CIG score} = \sum_{1}^{i} (\text{Coefi} \times \text{ExpGenei}).$$

Survival analysis based on the CIG score

The patients were divided into high-CIG and low-CIG score groups based on the median CIG score, and the Kaplan-Meier method was used to estimate the overall survival of the patients in the two groups.

Analysis of the predictive ability of the CIG score based on the internal and external validation datasets

The mUC patients in the IMvigor210 study were used as the internal validation dataset for CIG score validation. Alexandra et al.'s study also used the pretreatment tumor tissues of UC

patients receiving anti-PD-L1 treatment as the research object, so this dataset was used as the external validation dataset for CIG score validation [21]. The CIG score and other popular biomarkers were included in logistic regression models, receiver operating characteristic (ROC) curves were drawn, and the area under the curve (AUC) was calculated to estimate the predictive ability of these models. The "rms" and "pROC" packages in R software were used to draw ROC curves and to calculate the AUC values.

Analysis of the predictive ability of the expression panel of CXCL9, GBP5, and IFNG based on the external validation datasets

Since the other external validation datasets involved patients with different cancers and different immunotherapies, the coefficients of the three biomarkers in the CIG score may not be applicable to datasets of other cancer types. Therefore, the expression of CXCL9, GBP5, and IFNG was directly included in the logistic regression model to update the coefs, ROC curves were drawn, and AUC values were calculated to estimate the predictive ability of the model in different datasets while evaluating other popular biomarkers for comparison.

Pan-cancer analysis

To explore the underlying mechanisms of the predictive genes affecting the response to immunotherapy, the associations of the predictive genes with the tumor microenvironment (TME) and immune cell infiltration were analyzed in 33 cancers in the TCGA database. The "ESTIMATE" package of R software was used to calculate the stromal score (indicating the presence of stromal cells in tumor tissue), immune score (representing the infiltration of immune cells in tumor tissue), and tumor purity for each tumor sample. Then, the correlations of the potential predictive genes with the stromal score, immune score, and tumor purity were separately analyzed in 33 cancers by using Spearman correlation analysis, and only the results with $|R| > 0.5$ and $P < 0.001$ were recorded [23]. CIBERSORT, a deconvolution algorithm, was used in this study to estimate the proportions of 22 tumor-infiltrating immune cell subsets across all tumor samples. Then the correlations of the predictive genes with the 22 tumor-infiltrating lymphocyte subsets were analyzed by using Spearman correlation analysis in 33 cancers, retaining only the results with $|R| > 0.5$ and $P < 0.001$ [24]. The online analysis website TISIDB (http://cis.hku.hk/TISIDB/index.php) was used to explore the potential relationship between GBP5 expression and immunoinhibitors by using Spearman correlation analysis in 30 cancers in the TCGA database.

Results

Identification and functional enrichment of DEGs between responders and nonresponders to anti-PD-L1 treatment for metastatic urothelial cancer

The "limma" package of R software was used to identify DEGs between 167 PD patients and 25 CR patients in the IMvigor210 dataset. A total of 32 genes had an adjusted *P* value < 0.05 and were upregulated in CR patients, of which five genes (CXCL9, CXCL10, CXCL13, CCL5, and GBP5) had $|\log2\ FC| > 1$. The heatmap and correlation heatmap of the DEGs are shown in **Figure 1A**, **1B**. GO functional enrichment analysis showed which biological processes (BPs), cellular components (CCs), and molecular functions (MFs) the DEGs were involved in. The main BPs included cellular defence response, regulation of response to biotic stimulus, regulation of natural killer cell mediated cytotoxicity, regulation of natural killer cell mediated immunity, regulation of cell killing, positive regulation of response to external stimulus, cell killing, regulation of innate immune response, regulation of immune effector process, and natural killer cell mediated cytotoxicity. The DEGs were mainly enriched on the external side of the plasma membrane in the CC category. Among the MFs, the DEGs were primarily enriched in cytokine receptor binding, chemokine receptor binding, cytokine activity, chemokine activity, receptor ligand activity, signaling receptor activator activity, CCR chemokine receptor binding, CXCR chemokine receptor binding, G protein-coupled receptor binding, and promoter-specific chromatin binding (**Figure 1C**, **1D**). The KEGG pathway enrichment analysis showed that the DEGs were mainly enriched in natural killer cell mediated cytotoxicity, antigen processing and presentation, cytokine-cytokine receptor interaction, graft-versus-host disease, viral protein interaction with cytokine and cytokine receptor, chemokine signaling pathway, inflammatory

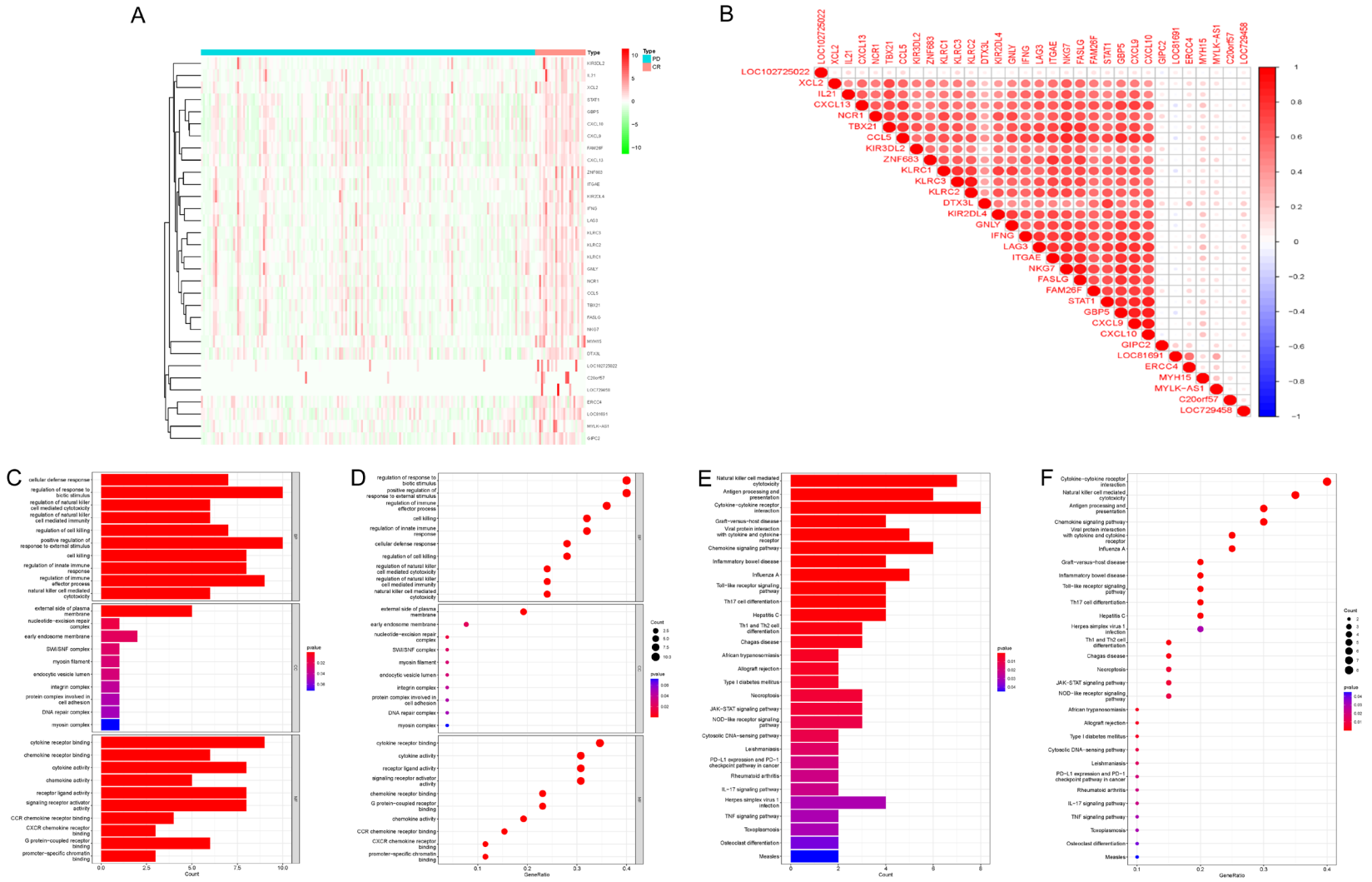

Figure 1. Identification and functional enrichment of DEGs between patients with complete response (CR) and those with progressive disease (PD) with anti-PD-L1 treatment of metastatic urothelial cancer. A. Heatmap of DEGs between CR patients and PD patients. B. Correlation heatmap of DEGs. C. Bar plot of GO functional enrichment of DEGs. D. Bubble plot of GO functional enrichment of DEGs. E. Bar plot of KEGG pathway enrichment of DEGs. F. Bubble plot of KEGG pathway enrichment of DEGs.

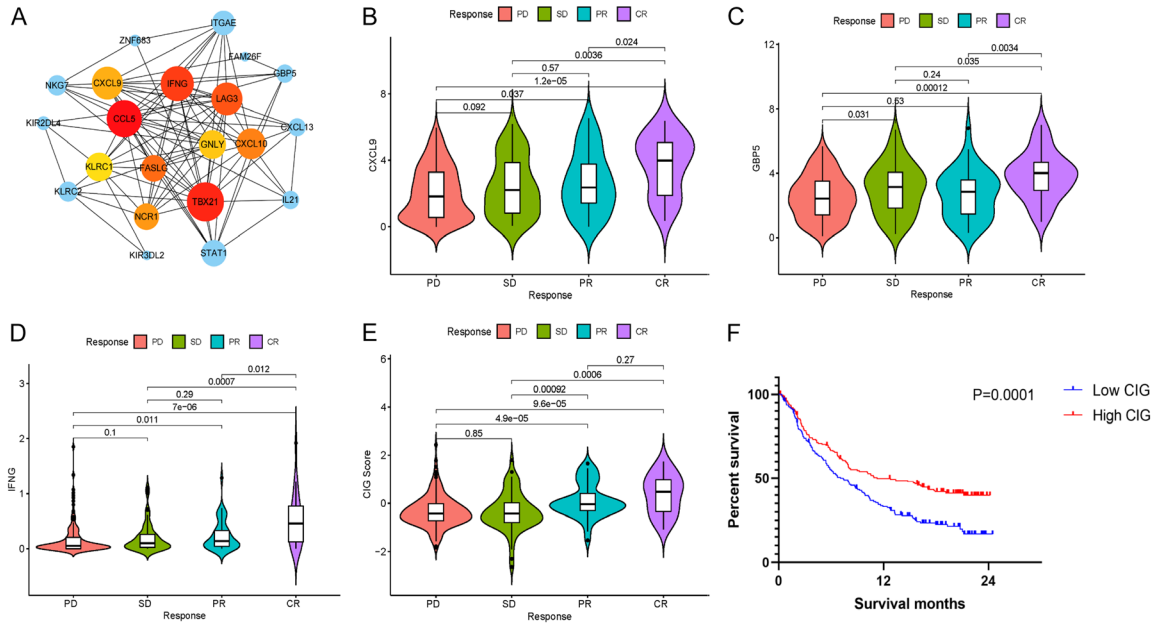

Figure 2. Identification of marker genes and establishment of the CIG score. A. The cytoHubba plug-in of Cytoscape was used to screen the top 10 hub genes among the differentially expressed genes according to the connectivity degree. B. Violin plot of CXCL9. C. Violin diagram of GBP5. D. Violin diagram of IFNG. E. Violin diagram of the CIG score. F. Overall survival curves of high- and low-CIG score patients.

Table 1. Multivariate logistic regression of the anti-PD-L1 immunotherapy response of candidate predictive genes

Gene	OR (95 CI%)	*P* value
CXCL13	1.142 (0.863, 1.512)	0.353
CXCL10	1.299 (0.850, 1.985)	0.227
CXCL9	1.775 (1.093, 2.882)	0.02
GBP5	0.358 (0.186, 0.690)	0.002
FASLG	0.295 (0.071, 1.230)	0.094
GNLY	1.324 (0.776, 2.259)	0.304
KLRC1	1.130 (0.469, 2.720)	0.786
LAG3	1.404 (0.605, 3.259)	0.429
TBX21	0.118 (0.011, 1.277)	0.079
CCL5	0.900 (0.512, 1.582)	0.714
NCR1	2.465 (0.914, 6.653)	0.075
IFNG	8.043 (1.525, 42.412)	0.014

bowel disease, influenza A, toll-like receptor signaling pathway, Th17-cell differentiation, hepatitis C, Th1 and Th2 cell differentiation, and Chagas disease (**Figure 1E**, **1F**).

Three candidate predictive genes independently associated with immunotherapy response

The DEGs were imported into the STRING online analysis website for PPI analysis. Then, the results of the PPI analysis were imported into Cytoscape software for visualization analysis, and the MCC value of each gene was calculated. The genes with the 10 highest MCC values were regarded as hub genes (**Figure 2A**). The hub genes and all DEGs with |log2 FC| > 1 (a total of 12 candidate predictive genes) were included in multivariate logistic regression analysis. The results showed that the expression of CXCL9, GBP5, and IFNG was independently associated with the immunotherapy response (**Table 1**).

Establishment and validation of the marker gene-derived CIG score

The expression of CXCL9, GBP5, and IFNG was included in multivariate logistic regression, the corresponding regression coefficients were obtained, and the CIG score was calculated as follows:

CIG score = Exp (CXCL9) × (0.6667) + Exp (GBP5) × (-0.7452) + Exp (IFNG) × (1.4092).

The distributions of CXCL9, GBP5, IFNG, and the CIG score among the different immunotherapy response groups are shown in **Figure 2B-E**. The patients were divided into low- and high-CIG score groups according to the median CIG score, and Kaplan-Meier analysis showed a sig-

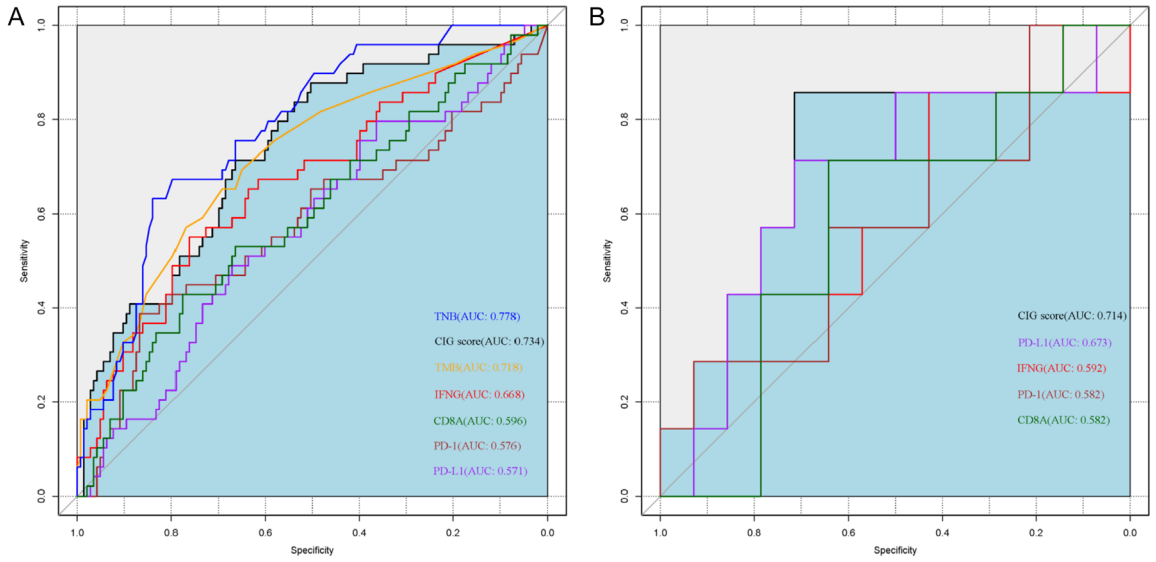

Figure 3. Internal and external validation of the CIG score. A. ROC curves based on the IMvigor210 dataset (training dataset). B. ROC curves based on Alexandra et al.'s dataset (external validation dataset).

nificant difference (P = 0.0001) in overall survival between the two groups (**Figure 2F**).

In the internal validation dataset, the ability of the CIG score (AUC: 0.734) to predict immunotherapy response ranked second among the popular biomarkers and was only second to TNB (AUC: 0.778) (**Figure 3A**). In Alexandra et. al.'s dataset, the predictive ability of the CIG score ranked first (AUC: 0.714) (**Figure 3B**).

Analysis of the potential mechanisms of the predictive genes affecting immunotherapy response in patients with mUC

Multinomial multivariate logistic regression analysis showed that the expression of GBP5 was associated with immune phenotypes, the expression of CXCL9 and GBP5 was associated with the immune cell level, and the expression of GBP5 and IFNG was associated with the tumor cell level (**Table 2**; **Figure 4A-E**). The expression levels of CXCL9, GBP5, and IFNG were all significantly correlated with TNB and TMB (**Figure 5A-F**).

Cross-cancer type validation of the ability of CXCL9, GBP5, and IFNG to predict the response to immunotherapy

A total of 13 immunotherapy datasets were used for external validation, and the characteristics of the datasets and AUC values for multiple biomarkers are shown in **Table 3** [12-20]. The expression of GBP5 was missing from the Chen et al., Prat et al. and PUCH datasets. The AUC values (CXCL9 + GBP5 + IFNG/CXCL9 + IFNG) were higher than those of PD-1, PD-L1, IFNG and CD8A in ten of the 13 datasets, higher than TMB in the datasets of Riaz et al. and Braun et al., and higher than TNB in the dataset of Riaz et al.

Pan-cancer analysis of the three biomarkers

The pan-cancer analysis based on the TCGA database showed that CXCL9 and GBP5 were positively correlated with the stromal score and the immune score but negatively correlated with tumor purity in multiple cancers (**Figure 6A**, **6B**). IFNG was mainly positively correlated with the immune score and negatively correlated with tumor purity in multiple cancers (**Figure 6C**). The pan-cancer analysis of the association of tumor immune cell infiltration revealed that CXCL9, GBP5, and IFNG were mainly positively correlated with the infiltration of M1 macrophages, activated memory CD4 T cells, and CD8 T cells in multiple cancers (**Figure 6D-F**).

The expression of GBP5 was strongly correlated with multiple immunosuppressive genes in cancers, and the results are shown in **Figure 7**.

Discussion

In this study, IFNG, CXCL9, and GBP5 were identified as biomarkers for predicting the

Table 2. Multinomial logistic regression of immune phenotype, immune cell level and tumor cell level in patients with metastatic urothelial cancer

Gene	Immunophenotype				
	Desert	Excluded		Inflamed	
		OR (95% CI)	*P* Value	OR (95% CI)	*P* Value
CXCL9	Reference	1.209 (0.727, 2.009)	0.465	1.314 (0.728, 2.373)	0.364
GBP5		2.594 (1.469, 4.581)	0.001	5.938 (2.868, 12.295)	< 0.001
IFNG		0.217 (0.009, 5.137)	0.344	1.309 (0.047, 36.181)	0.874
	Immune cell level				
	IC0	IC1		IC2+	
		OR (95% CI)	*P* Value	OR (95% CI)	*P* Value
CXCL9	Reference	0.935 (0.581, 1.505)	0.781	1.984 (1.193, 3.301)	0.008
GBP5		2.740 (1.656, 4.534)	< 0.001	2.403 (1.357, 4.255)	0.003
IFNG		1.030 (0.054, 19.642)	0.984	1.368 (0.069, 26.927)	0.837
	Tumor cell level				
	TC0	TC1		TC2+	
		OR (95% CI)	*P* Value	OR (95% CI)	*P* Value
CXCL9	Reference	1.242 (0.700, 2.203)	0.459	1.036 (0.725, 1.480)	0.848
GBP5		0.638 (0.312, 1.304)	0.218	2.033 (1.294, 3,195)	0.002
IFNG		7.498 (1.279, 43.954)	0.026	1.377 (0.369, 5.148)	0.634

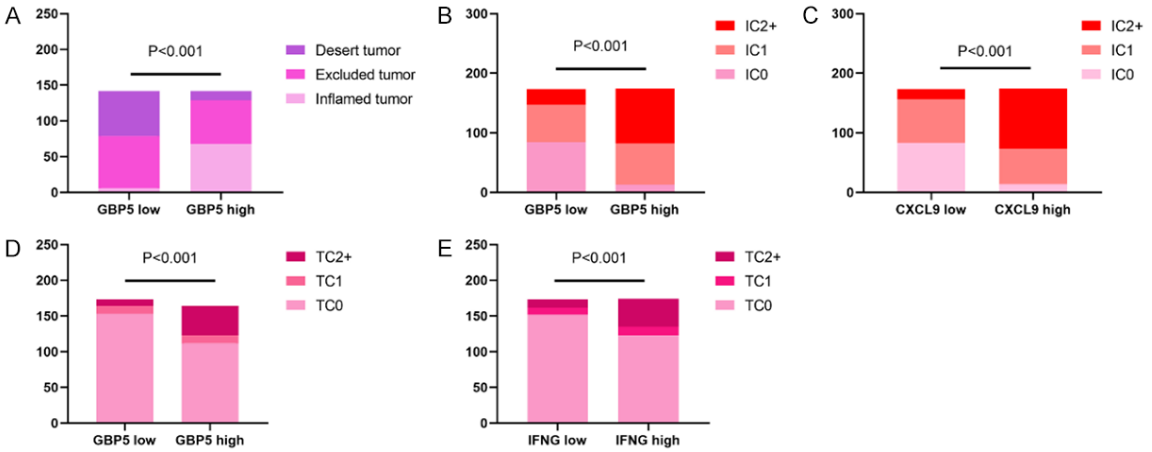

Figure 4. Correlation of the predictive genes with the tumor immunophenotype, immune cell level, and tumor cell (TC) level (Chi square test). A. Bar graph of the correlation between the expression of GBP5 and immunophenotype. B. Bar graph of the correlation between the expression of GBP5 and the immune cell (IC) level. C. Bar graph of the correlation between the expression of CXCL9 and the IC level. D. Bar graph of the correlation between the expression of GBP5 and the TC level. E. Bar graph of the correlation between the expression of IFNG and the TC level.

response to anti-PD-L1 immunotherapy in mUC patients. The ability of the panel of CXCL9, GBP5, and IFNG to predict immunotherapy response was also validated in multiple immunotherapy datasets of different cancers and was superior to that of IFNG, PD-1, PD-L1, CD8A, TMB and TNB.

Many factors may influence the efficacy of immunotherapy, and differences in both tumor and clinical characteristics among cancer patients result in only a subset of patients benefiting from immunotherapy [25, 26]. Therefore, finding effective biomarkers to predict immunotherapy response in cancer patients is of great importance for regimen selection. ICIs enhance the immune response of the immune system against tumors by blocking immune checkpoints, so whether patients can respond to ICIs depends on whether the immune system can

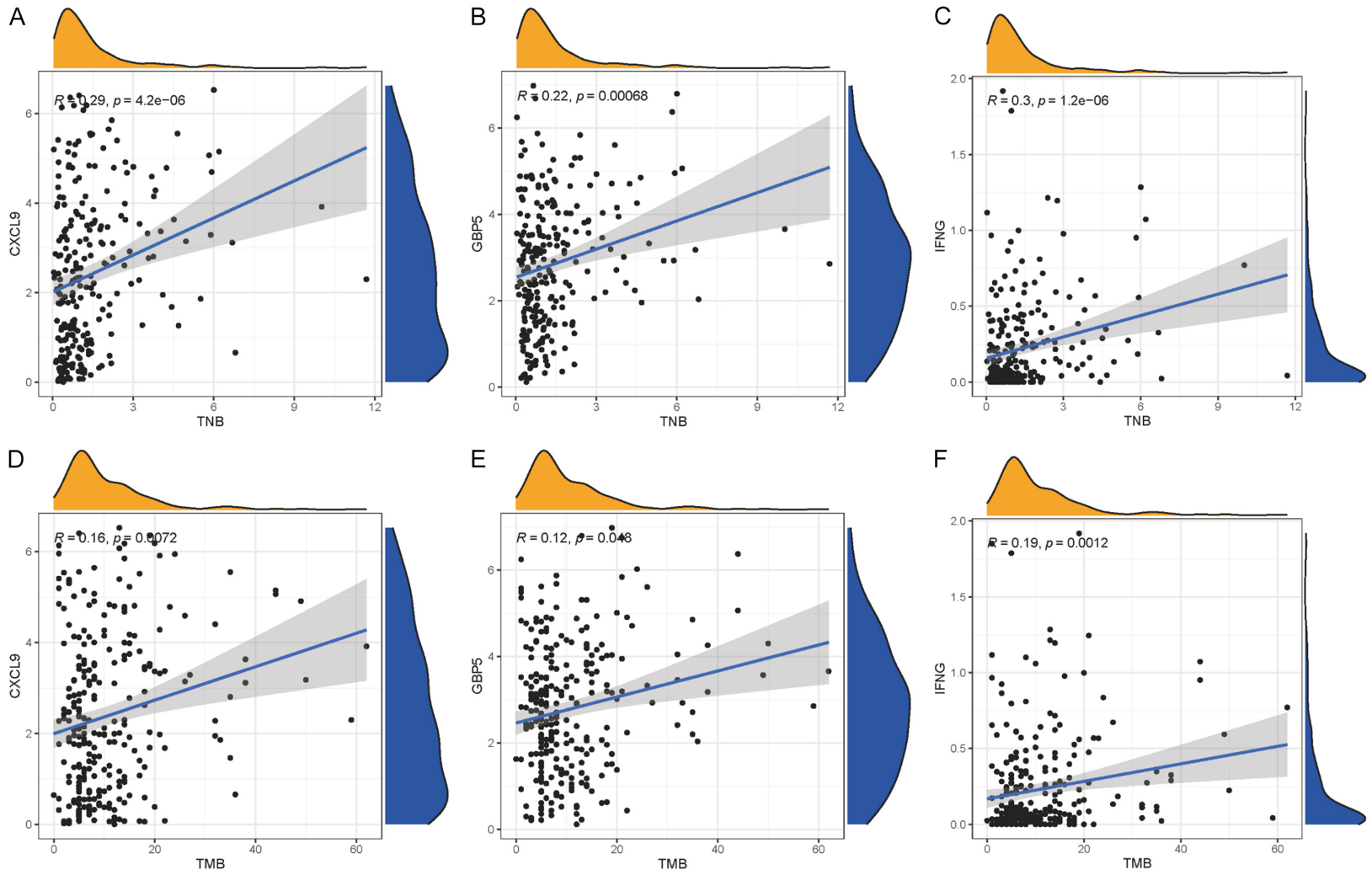

Figure 5. Correlation of the predictive genes with tumor neoantigen burden (TNB) and tumor mutational burden (TMB). A. Scatter plot of the correlations for CXCL9 and TNB. B. Scatter plot of the correlations for GBP5 and TNB. C. Scatter plot of the correlations for IFNG and TNB. D. Scatter plot of the correlations for CXCL9 and TMB. E. Scatter plot of the correlations for GBP5 and TMB. F. Scatter plot of the correlations for IFNG and TMB.

Table 3. Predictive ability of multiple biomarkers for immunotherapy response across the external validation datasets

Study	Number of patients	Cancer	AUC (CXCL9 + GBP5 + IFNG)	AUC (CXCL9 + IFNG)	AUC (IFNG)	AUC (PD-1)	AUC (PD-L1)	AUC (CD8A)	AUC (TMB)	AUC (TNB)
Nathanson et al. CTLA4	9	SKCM	1 (1)	0.950 (2)	0.75 (3)	0.600 (5)	0.650 (4)	0.450 (6)	-	-
Kim et al. PD-1	45	STAD	0.843 (1)	0.843 (1)	0.843 (1)	0.763 (4)	0.833 (2)	0.798 (3)	-	-
Gide et al. PD-1	41	SKCM	0.816 (5)	0.811 (6)	0.837 (2)	0.849 (1)	0.828 (3)	0.818 (4)	-	-
Gide et al. PD-1 + CTLA4	32	SKCM	0.81 (1)	0.805 (2)	0.738 (4)	0.658 (6)	0.788 (3)	0.736 (5)	-	-
Lauss et al. ACT	25	SKCM	0.787 (1)	0.727 (3)	0.72 (4)	0.687 (5)	0.733 (2)	0.680 (6)	-	-
Riaz et al. PD-1 + CTLA4	44	SKCM	0.690 (1)	0.631 (4)	0.603 (6)	0.651 (3)	0.541 (8)	0.656 (2)	0.574 (7)	0.609 (5)
Braun et al. PD-1	172	KIRC	0.587 (1)	0.541 (3)	0.541 (3)	0.496 (5)	0.569 (2)	0.492 (6)	0.511 (4)	-
Hugo et al. PD-1	26	SKCM	0.56 (2)	0.530 (5)	0.542 (4)	0.548 (3)	0.601 (1)	0.530 (5)	-	-
PUCH PD-L1	14	GI	-	0.875 (1)	0.833 (2)	0.792 (3)	0.750 (4)	0.542 (5)	-	-
Chen et al. CTLA4 + PD-1	14	SKCM	-	0.822 (1)	0.8 (2)	0.733 (3)	0.622 (4)	0.8 (2)	-	-
Chen et al. CTLA4	16	SKCM	-	0.673 (1)	0.509 (4)	0.582 (3)	0.582 (3)	0.636 (2)	-	-
Prat et al. PD-1	33	NSLC + HNSC + SKCM	-	0.671 (1)	0.569 (3)	0.635 (2)	0.417 (4)	0.635 (2)	-	-
PUCH PD-1	61	GI	-	0.653 (3)	0.677 (2)	0.619 (4)	0.719 (1)	0.585 (5)	-	-

SKCM, skin cutaneous melanoma; STAD, stomach adenocarcinoma; KIRC, kidney renal clear cell carcinoma; GI, gastrointestinal cancer; NSLC, non-small cell lung cancer; HNSC, head and neck squamous cell carcinoma.

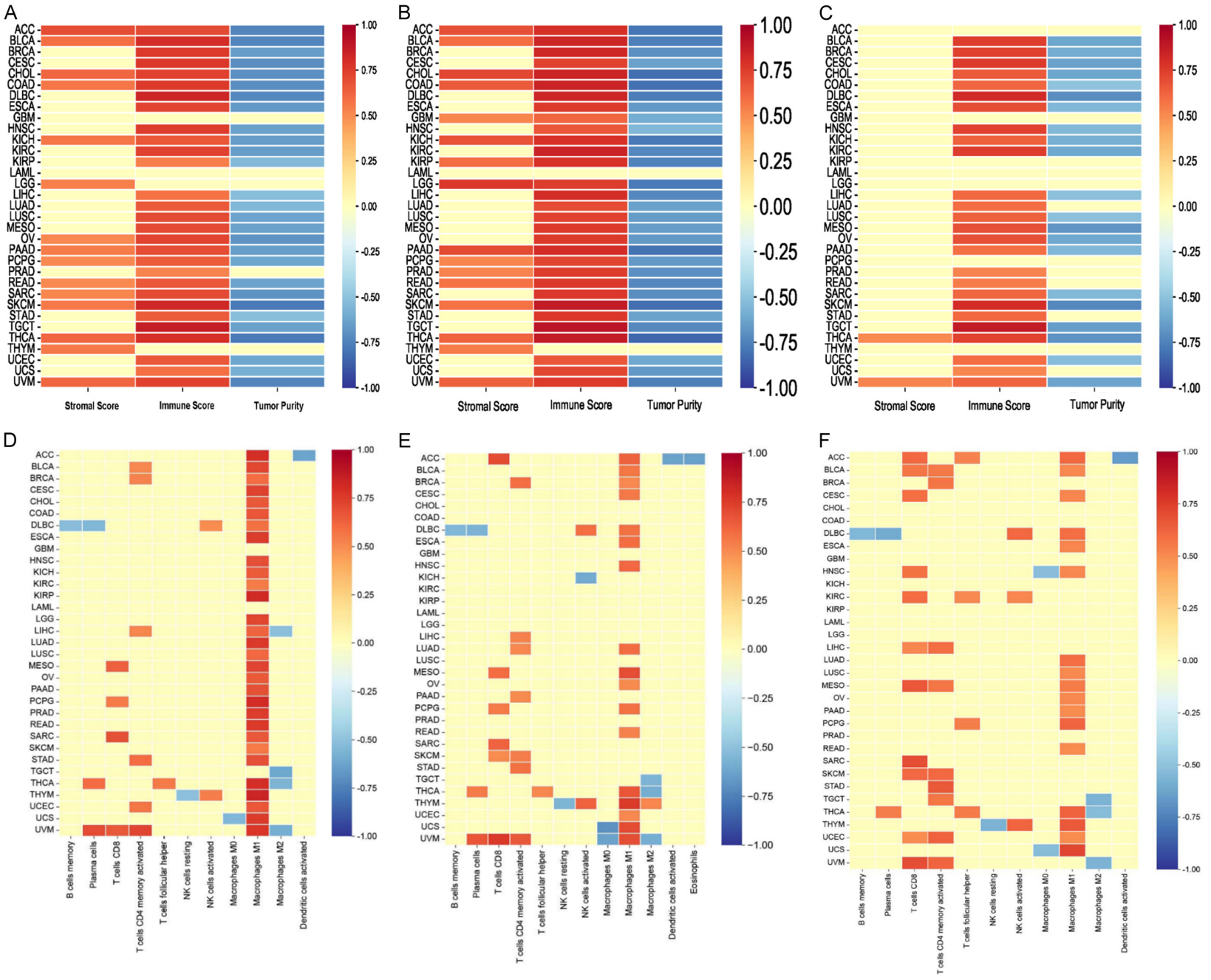
A
B
C
D
E
F
ACC
BLCA
BRCA
CESC
CHOL
COAD
DLBC
ESCA
GBM
HNSC
KICH
KIRC
KIRP
LAML
LGG
LIHC
LUAD
LUSC
MESO
OV
PAAD
PCPG
PRAD
READ
SARC
SKCM
STAD
TGCT
THCA
THYM
UCEC
UCS
UVM
Stromal Score
Immune Score
Tumor Purity
1.00
0.75
0.50
0.25
0.00
-0.25
-0.50
-0.75
-1.00
B cells memory
Plasma cells
T cells CD8
T cells CD4 memory activated
T cells follicular helper
NK cells resting
NK cells activated
Macrophages M0
Macrophages M1
Macrophages M2
Dendritic cells activated
Eosinophils

Figure 6. Pan-cancer analysis of the correlation of the predictive genes with tumour components and immune cell infiltration. A. Correlation heatmap of CXCL9 expression with tumor components. B. Correlation heatmap of GBP5 expression with tumor components. C. Correlation heatmap of IFNG expression with tumor components. D. Correlation heatmap of CXCL9 expression with immune cell infiltration. E. Correlation heatmap of GBP5 expression with immune cell infiltration. F. Correlation heatmap of IFNG expression with immune cell infiltration.

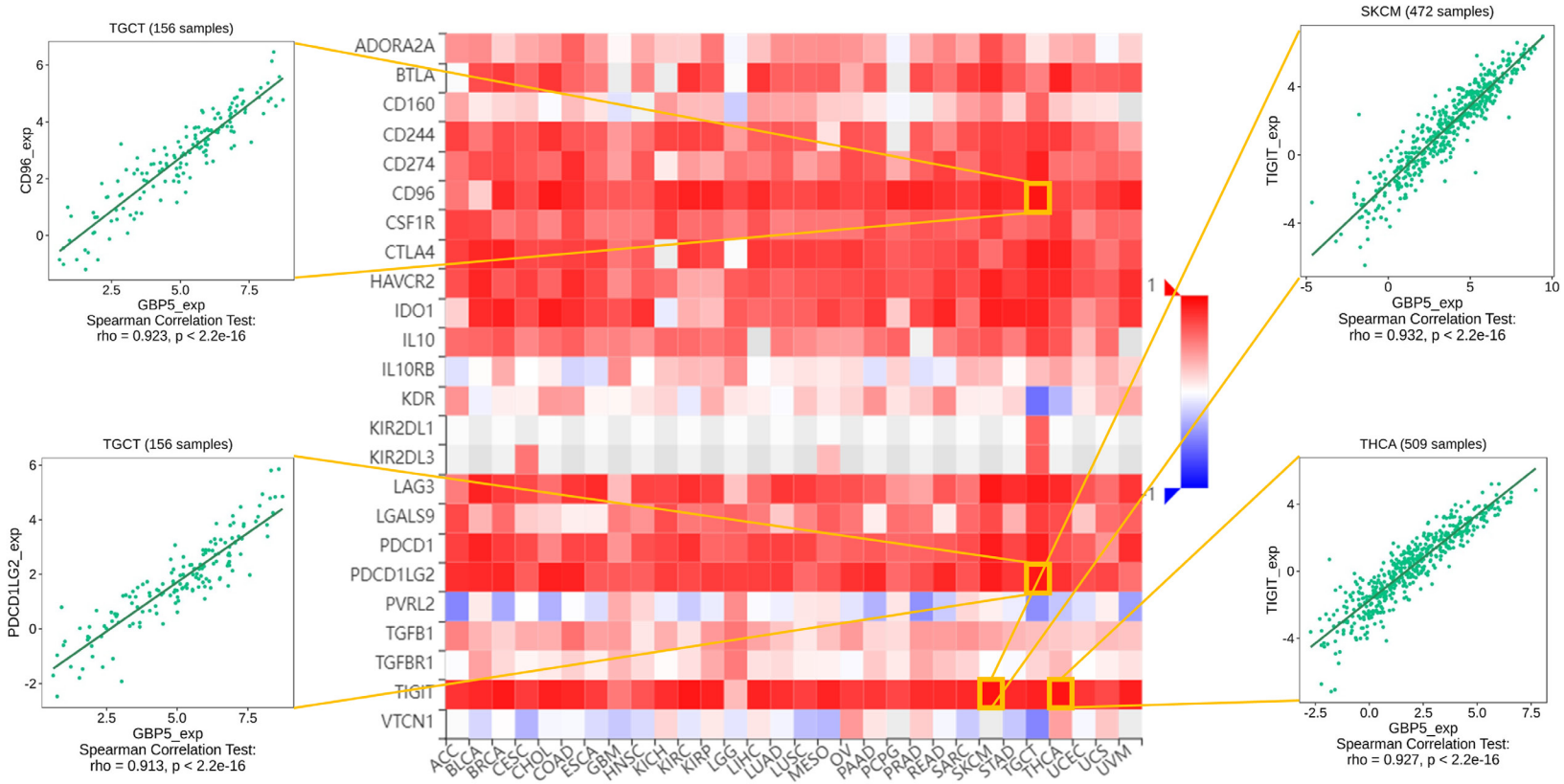

Figure 7. Correlation heatmap of GBP5 with immunoinhibitors. The top 4 strongest associations are displayed by using dot plots.

recognize tumor cells and generate an immune response. Current biomarkers predict immunotherapy response mainly through three strategies: the first is assessing the neoantigen level of tumor cells to predict whether tumor cells can be recognized by immune cells; the second is to infer whether the immune system has generated an immune response against the tumor cells by measuring the levels of specific immune cells or inflammatory factors within the tumor tissues; and the third is using the expression of specific immune checkpoints within tumor tissues to reflect the level of immunosuppressive environment. Based on the above strategies, multiple emerging biomarkers have been extensively studied and discussed, including PD-L1, IFN-γ, TMB, TNB, microsatellite instability (MSI), CD8+ T cells, mutations in JAK, MDM2/MDM4, EGFR, etc [10, 27]. This study also confirmed that IFN-γ played an essential role in predicting the response to immunotherapy. The production of IFN-γ is mainly regulated by natural killer (NK) and natural killer T (NKT) cells in innate immunity, and CD8+ and CD4+ T cells are primary paracrine sources of IFN-γ during adaptive immune responses. Upon stimulation by tumor cell neoantigens, these cells activate adaptive immunity against cancer cells through the production of IFN-γ [28, 29]. Therefore, the expression of IFN-γ within tumor tissue can indicate, to some extent, whether the immune system can recognize tumor cells as abnormal cells and provoke an immune response. The results of the DEG analysis in this study showed that IFN-γ and its downstream genes were highly expressed in patients with CR, providing further evidence that IFN-γ is an important feature of tumor immunity. The level of IFN-γ within the tumor mass can also influence the magnitude of the tumor immune response, and intravesical Bacillus Calmette Guérin (BCG) immunotherapy, a treatment for noninvasive bladder cancers, works by inducing the production of IFN-γ and other inflammatory factors [29, 30]. Of note, the expression of PD-L1 is widely discussed as a potential biomarker for predicting the response to anti-PD-1 or anti-PD-L1 immunotherapy. However, in the analysis of DEGs in this study, PD-L1 was not differentially expressed in pretreatment tumor tissues between CR patients and PD patients, so it seems insufficient to use PD-L1 as a sole biomarker for predicting the response to anti-PD-L1 or anti-PD-1 immunotherapy [31].

In this study, the expression of CXCL9 was also identified as an independent influencing factor of immunotherapy response. Based on current studies, CXCL9 is mainly secreted by monocytes, endothelial cells, fibroblasts and cancer cells in response to IFN-γ; thus, its expression level is closely related to tumor components [32]. Herbst et al.'s study also showed that CXCL9 was highly expressed in the pretreatment tumor tissues of anti-PD-L1 melanoma responders; however, this association was weaker in non-small cell lung cancer and renal cell carcinoma patients, and this difference may be due to differences in the tumor components of different cancers [33]. Although CXCL9 is not highly expressed in responders to immunotherapy in all cancers, its role in predicting the response to immunotherapy should not be neglected, and its function is mainly involved in mediating lymphocyte infiltration and the differentiation and activation of immune cells to inhibit tumor growth [32]. The internal analysis and pan-cancer analysis of this study showed similar results that CXCL9 was significantly correlated with immune cell infiltration, especially CD4+ T cells, CD8+ T cells, and M1 macrophages. A study by Chow et al. showed that tumor-bearing mice lacking CXCR3, the receptor for CXCL9, respond poorly to anti-PD-1 therapy and that CXCR3 and its ligand CXCL9 are essential for the generation of CD8+ T-cell responses in tumor-bearing mice treated with anti-PD-1 therapy [34].

Based on the results, GBP5 had a negative coefficient in the CIG score formula, and it apparently played a negative role in tumor immunity in patients treated with anti-PD-L1 immunotherapy. The immunosuppressive effect of GBP5 may be achieved through the regulation of the expression of immunoinhibitors and pan-cancer analysis revealed a strong correlation between the expression of GBP5 and multiple immunoinhibitors in 30 cancers. In addition, a study on triple-negative breast cancer showed that GBP5 could regulate PD-L1 expression in tumor cells and is associated with the migration ability of tumor cells [35]. Our results also showed a significant association between GBP5 and the immunophenotype of patients with mUC. Therefore, GBP5 may also have a regulatory relationship with the expression of other immunoinhibitors, and high expression of multiple immunoinhibitors may

negatively affect the efficacy of immunotherapy with a single target. The immunosuppressive effects of GBP5 may also be achieved by regulating the assembly of the NLRP3 inflammasome [36]. To date, several studies have shown that the NLRP3 inflammasome has a close relationship with the TME and tumor progression [37-39]. Ju et al. showed that the NLRP3 inflammasome was significantly associated with immune checkpoint expression in 15 cancers [40]. A study by Wang et al. indicated that NLRP3 mutations were associated with elevated TMB, favorable immune infiltration, and better ICI efficacy [39]. A study on breast cancer demonstrated that the cancer-associated fibroblast-derived NLRP3 inflammasome can modulate the TME toward an immunosuppressive environment and upregulate the expression of adhesion molecules on endothelial cells to promote tumor progression and metastasis [41]. However, the specific role of the NLRP3 inflammasome in the process of tumor immunity still needs further research to clarify.

Based on the current evidence, it seems that a single biomarker is not sufficient to accurately predict the response of cancer patients to immunotherapy. The strength of tumor immunity in patients is regulated by different positive and negative factors and is in an individualized equilibrium, so the combined expression of different genes to predict immunotherapy response seems to be a more effective strategy. Furthermore, in addition to the characteristics of the tumor, it seems that the state of the patient's immune system should also be considered an important factor in predicting the response to immunotherapy, and several studies have demonstrated that worse performance status is associated with a poor immunotherapy response [42-45]. Predicting immunotherapy response using a combination of multiple indicators is being increasingly implemented [46].

This study has the following limitations. First, five of the 14 validation datasets lacked data on the expression of GBP5, resulting in the inability to validate the predictive ability of the expression panel of CXCL9, IFNG, and GBP5. Second, the tumor samples involved in the data from PUCH were biopsy samples, which were quite limited and not enough to further complete basic experiments such as immunohistochemistry to validate the results.

Conclusion

This study found that the expression panel of CXCL9, GBP5, and IFNG in tumor tissues can potentially be used as a pan-cancer predictive biomarker for immunotherapy response.

Acknowledgements

We thank Dr. Deng Jingwen for her valuable comments on this study. This study was supported by the China Scholarship Council (2020-07040025), Clinical Medicine Plus X - Young Scholars Project of Peking University (PKU-2022LCXQ038), and Fundamental Research Funds for the Central Universities and the Science Foundation of Peking University Cancer Hospital (KC2210).

Disclosure of conflict of interest

None.

Address correspondence to: Zhouqiao Wu, Ward I of Gastrointestinal Cancer Center, Key Laboratory of Carcinogenesis and Translational Research (Ministry of Education), Peking University Cancer Hospital and Institute, Beijing 100142, China. E-mail: wuzhouqiao@gmail.com

References

[1] Kono K, Nakajima S and Mimura K. Current status of immune checkpoint inhibitors for gastric cancer. Gastric Cancer 2020; 23: 565-578.

[2] Sabbatino F, Liguori L, Pepe S and Ferrone S. Immune checkpoint inhibitors for the treatment of melanoma. Expert Opin Biol Ther 2022; 22: 563-576.

[3] Soh J, Hamada A, Fujino T and Mitsudomi T. Perioperative therapy for non-small cell lung cancer with immune checkpoint inhibitors. Cancers (Basel) 2021; 13: 4035.

[4] Lopez-Beltran A, Cimadamore A, Blanca A, Massari F, Vau N, Scarpelli M, Cheng L and Montironi R. Immune checkpoint inhibitors for the treatment of bladder cancer. Cancers (Basel) 2021; 13: 131.

[5] Johnson DB, Sullivan RJ and Menzies AM. Immune checkpoint inhibitors in challenging populations. Cancer 2017; 123: 1904-1911.

[6] Ohaegbulam KC, Assal A, Lazar-Molnar E, Yao Y and Zang X. Human cancer immunotherapy with antibodies to the PD-1 and PD-L1 pathway. Trends Mol Med 2015; 21: 24-33.

[7] Wang D, Sun K, Wang T, Zhang D, Sun F, Cui Y, Zhao H and Wu J. Adverse effects and toxicity

of immune checkpoint inhibitors for patients with urothelial carcinoma. Front Pharmacol 2021; 12: 710943.

[8] Montisci A, Vietri MT, Palmieri V, Sala S, Donatelli F and Napoli C. Cardiac toxicity associated with cancer immunotherapy and biological drugs. Cancers 2021; 13: 4797.

[9] Berner F, Bomze D, Diem S, Ali OH, Fässler M, Ring S, Niederer R, Ackermann CJ, Baumgaertner P, Pikor N, Cruz CG, van de Veen W, Akdis M, Nikolaev S, Läubli H, Zippelius A, Hartmann F, Cheng HW, Hönger G, Recher M, Goldman J, Cozzio A, Früh M, Neefjes J, Driessen C, Ludewig B, Hegazy AN, Jochum W, Speiser DE and Flatz L. Association of checkpoint inhibitor-induced toxic effects with shared cancer and tissue antigens in non-small cell lung cancer. JAMA Oncol 2019; 5: 1043-1047.

[10] Gibney GT, Weiner LM and Atkins MB. Predictive biomarkers for checkpoint inhibitor-based immunotherapy. Lancet Oncol 2016; 17: e542-e551.

[11] Mariathasan S, Turley SJ, Nickles D, Castiglioni A, Yuen K, Wang Y, Kadel EE III, Koeppen H, Astarita JL, Cubas R, Jhunjhunwala S, Banchereau R, Yang Y, Guan Y, Chalouni C, Ziai J, Şenbabaoğlu Y, Santoro S, Sheinson D, Hung J, Giltnane JM, Pierce AA, Mesh K, Lianoglou S, Riegler J, Carano RAD, Eriksson P, Höglund M, Somarriba L, Halligan DL, van der Heijden MS, Loriot Y, Rosenberg JE, Fong L, Mellman I, Chen DS, Green M, Derleth C, Fine GD, Hegde PS, Bourgon R and Powles T. TGFβ attenuates tumour response to PD-L1 blockade by contributing to exclusion of T cells. Nature 2018; 554: 544-548.

[12] Braun DA, Hou Y, Bakouny Z, Ficial M, Sant' Angelo M, Forman J, Ross-Macdonald P, Berger AC, Jegede OA, Elagina L, Steinharter J, Sun M, Wind-Rotolo M, Pignon JC, Cherniack AD, Lichtenstein L, Neuberg D, Catalano P, Freeman GJ, Sharpe AH, McDermott DF, Van Allen EM, Signoretti S, Wu CJ, Shukla SA and Choueiri TK. Interplay of somatic alterations and immune infiltration modulates response to PD-1 blockade in advanced clear cell renal cell carcinoma. Nat Med 2020; 26: 909-918.

[13] Chen PL, Roh W, Reuben A, Cooper ZA, Spencer CN, Prieto PA, Miller JP, Bassett RL, Gopalakrishnan V, Wani K, De Macedo MP, Austin-Breneman JL, Jiang H, Chang Q, Reddy SM, Chen WS, Tetzlaff MT, Broaddus RJ, Davies MA, Gershenwald JE, Haydu L, Lazar AJ, Patel SP, Hwu P, Hwu WJ, Diab A, Glitza IC, Woodman SE, Vence LM, Wistuba II, Amaria RN, Kwong LN, Prieto V, Davis RE, Ma W, Overwijk WW, Sharpe AH, Hu J, Futreal PA, Blando J, Sharma P, Allison JP, Chin L and Wargo JA. Analysis of immune signatures in longitudinal tumor samples yields insight into biomarkers of response and mechanisms of resistance to immune checkpoint blockade. Cancer Discov 2016; 6: 827-837.

[14] Gide TN, Quek C, Menzies AM, Tasker AT, Shang P, Holst J, Madore J, Lim SY, Velickovic R, Wongchenko M, Yan Y, Lo S, Carlino MS, Guminski A, Saw RPM, Pang A, McGuire HM, Palendira U, Thompson JF, Rizos H, Silva IPD, Batten M, Scolyer RA, Long GV and Wilmott JS. Distinct immune cell populations define response to Anti-PD-1 monotherapy and Anti-PD-1/Anti-CTLA-4 combined therapy. Cancer Cell 2019; 35: 238-255, e6.

[15] Hugo W, Zaretsky JM, Sun L, Song C, Moreno BH, Hu-Lieskovan S, Berent-Maoz B, Pang J, Chmielowski B, Cherry G, Seja E, Lomeli S, Kong X, Kelley MC, Sosman JA, Johnson DB, Ribas A and Lo RS. Genomic and transcriptomic features of response to Anti-PD-1 therapy in metastatic melanoma. Cell 2016; 165: 35-44.

[16] Lauss M, Donia M, Harbst K, Andersen R, Mitra S, Rosengren F, Salim M, Vallon-Christersson J, Törngren T, Kvist A, Ringnér M, Svane IM and Jönsson G. Mutational and putative neoantigen load predict clinical benefit of adoptive T cell therapy in melanoma. Nat Commun 2017; 8: 1738.

[17] Nathanson T, Ahuja A, Rubinsteyn A, Aksoy BA, Hellmann MD, Miao D, Van Allen E, Merghoub T, Wolchok JD, Snyder A and Hammerbacher J. Somatic mutations and neoepitope homology in melanomas treated with CTLA-4 blockade. Cancer Immunol Res 2017; 5: 84-91.

[18] Prat A, Navarro A, Paré L, Reguart N, Galván P, Pascual T, Martínez A, Nuciforo P, Comerma L, Alos L, Pardo N, Cedrés S, Fan C, Parker JS, Gaba L, Victoria I, Viñolas N, Vivancos A, Arance A and Felip E. Immune-related gene expression profiling after PD-1 blockade in non-small cell lung carcinoma, head and neck squamous cell carcinoma, and melanoma. Cancer Res 2017; 77: 3540-3550.

[19] Riaz N, Havel JJ, Makarov V, Desrichard A, Urba WJ, Sims JS, Hodi FS, Martín-Algarra S, Mandal R, Sharfman WH, Bhatia S, Hwu WJ, Gajewski TF, Slingluff CL Jr, Chowell D, Kendall SM, Chang H, Shah R, Kuo F, Morris LGT, Sidhom JW, Schneck JP, Horak CE, Weinhold N and Chan TA. Tumor and microenvironment evolution during immunotherapy with nivolumab. Cell 2017; 171: 934-949, e916.

[20] Kim ST, Cristescu R, Bass AJ, Kim KM, Odegaard JI, Kim K, Liu XQ, Sher X, Jung H, Lee M, Lee S, Park SH, Park JO, Park YS, Lim HY, Lee H, Choi M, Talasaz A, Kang PS, Cheng J, Loboda A, Lee J and Kang WK. Comprehensive molecular characterization of clinical responses to PD-1 inhibition in metastatic gastric cancer. Nat Med 2018; 24: 1449-1458.

[21] Snyder A, Nathanson T, Funt SA, Ahuja A, Buros Novik J, Hellmann MD, Chang E, Aksoy BA, Al-Ahmadie H, Yusko E, Vignali M, Benzeno S, Boyd M, Moran M, Iyer G, Robins HS, Mardis ER, Merghoub T, Hammerbacher J, Rosenberg JE and Bajorin DF. Contribution of systemic and somatic factors to clinical response and resistance to PD-L1 blockade in urothelial cancer: an exploratory multi-omic analysis. PLoS Med 2017; 14: e1002309.

[22] Chin CH, Chen SH, Wu HH, Ho CW, Ko MT and Lin CY. cytoHubba: identifying hub objects and sub-networks from complex interactome. BMC Syst Biol 2014; 8 Suppl 4: S11.

[23] Yoshihara K, Shahmoradgoli M, Martínez E, Vegesna R, Kim H, Torres-Garcia W, Treviño V, Shen H, Laird PW, Levine DA, Carter SL, Getz G, Stemke-Hale K, Mills GB and Verhaak RG. Inferring tumour purity and stromal and immune cell admixture from expression data. Nat Commun 2013; 4: 2612.

[24] Newman AM, Liu CL, Green MR, Gentles AJ, Feng W, Xu Y, Hoang CD, Diehn M and Alizadeh AA. Robust enumeration of cell subsets from tissue expression profiles. Nat Methods 2015; 12: 453-457.

[25] Wang S, He Z, Wang X, Li H and Liu XS. Antigen presentation and tumor immunogenicity in cancer immunotherapy response prediction. Elife 2019; 8: e49020.

[26] Duffy MJ and Crown J. Biomarkers for predicting response to immunotherapy with immune checkpoint inhibitors in cancer patients. Clin Chem 2019; 65: 1228-1238.

[27] Sholl LM. Biomarkers of response to checkpoint inhibitors beyond PD-L1 in lung cancer. Mod Pathol 2022; 35: 66-74.

[28] Jorgovanovic D, Song M, Wang L and Zhang Y. Roles of IFN-γ in tumor progression and regression: a review. Biomark Res 2020; 8: 49-49.

[29] Kursunel MA and Esendagli G. The untold story of IFN-γ in cancer biology. Cytokine Growth Factor Rev 2016; 31: 73-81.

[30] Zheng YQ, Naguib YW, Dong Y, Shi YC, Bou S and Cui Z. Applications of bacillus Calmette-Guerin and recombinant bacillus Calmette-Guerin in vaccine development and tumor immunotherapy. Expert Rev Vaccines 2015; 14: 1255-1275.

[31] Doroshow DB, Bhalla S, Beasley MB, Sholl LM, Kerr KM, Gnjatic S, Wistuba, II, Rimm DL, Tsao MS and Hirsch FR. PD-L1 as a biomarker of response to immune-checkpoint inhibitors. Nat Rev Clin Oncol 2021; 18: 345-362.

[32] Tokunaga R, Zhang W, Naseem M, Puccini A, Berger MD, Soni S, McSkane M, Baba H and Lenz HJ. CXCL9, CXCL10, CXCL11/CXCR3 axis for immune activation-a target for novel cancer therapy. Cancer Treat Rev 2018; 63: 40-47.

[33] Herbst RS, Soria JC, Kowanetz M, Fine GD, Hamid O, Gordon MS, Sosman JA, McDermott DF, Powderly JD, Gettinger SN, Kohrt HEK, Horn L, Lawrence DP, Rost S, Leabman M, Xiao Y, Mokatrin A, Koeppen H, Hegde PS, Mellman I, Chen DS and Hodi FS. Predictive correlates of response to the anti-PD-L1 antibody MPDL3280A in cancer patients. Nature 2014; 515: 563-567.

[34] Chow MT, Ozga AJ, Servis RL, Frederick DT, Lo JA, Fisher DE, Freeman GJ, Boland GM and Luster AD. Intratumoral activity of the CXCR3 chemokine system is required for the efficacy of anti-PD-1 therapy. Immunity 2019; 50: 1498-1512, e5.

[35] Cheng SW, Chen PC, Lin MH, Ger TR, Chiu HW and Lin YF. GBP5 repression suppresses the metastatic potential and PD-L1 expression in triple-negative breast cancer. Biomedicines 2021; 9: 371.

[36] Shenoy AR, Wellington DA, Kumar P, Kassa H, Booth CJ, Cresswell P and MacMicking JD. GBP5 promotes NLRP3 inflammasome assembly and immunity in mammals. Science 2012; 336: 481-485.

[37] Gouravani M, Khalili N, Razi S, Keshavarz-Fathi M, Khalili N and Rezaei N. The NLRP3 inflammasome: a therapeutic target for inflammation-associated cancers. Expert Rev Clin Immunol 2020; 16: 175-187.

[38] Theivanthiran B, Haykal T, Cao L, Holtzhausen A, Plebanek M, DeVito NC and Hanks BA. Overcoming immunotherapy resistance by targeting the tumor-intrinsic NLRP3-HSP70 signaling axis. Cancers 2021; 13: 4753.

[39] Wang Q, Lyu J, Zhang W, Shi F, Ren Y, Mao Q, Liu Y, Li Y and Wang S. Immunological and clinical immunotherapy implications of NLRP3 mutations in melanoma. Aging 2021; 13: 24271-24289.

[40] Ju M, Bi J, Wei Q, Jiang L, Guan Q, Zhang M, Song X, Chen T, Fan J, Li X, Wei M and Zhao L. Pan-cancer analysis of NLRP3 inflammasome with potential implications in prognosis and immunotherapy in human cancer. Brief Bioinform 2021; 22: bbaa345.

[41] Ershaid N, Sharon Y, Doron H, Raz Y, Shani O, Cohen N, Monteran L, Leider-Trejo L, Ben-Shmuel A, Yassin M, Gerlic M, Ben-Baruch A, Pasmanik-Chor M, Apte R and Erez N. NLRP3 inflammasome in fibroblasts links tissue damage with inflammation in breast cancer progression and metastasis. Nat Commun 2019; 10: 4375.

[42] Tomasik B, Bieńkowski M, Braun M, Popat S and Dziadziuszko R. Effectiveness and safety of immunotherapy in NSCLC patients with ECOG PS score ≥2 - systematic review and meta-analysis. Lung Cancer 2021; 158: 97-106.

[43] Cybulska-Stopa B, Pacholczak-Madej R, Kamińska-Winciorek G, Ziętek M, Czarnecka AM, Piejko K, Galus Ł, Ziółkowska B, Kieszko S, Kempa-Kamińska N, Calik J, Rolski J, Sałek-Zań A, Gajewska-Wicher K, Drosik-Kwaśniewska A, Rogala P, Kubiatowski T, Suwiński R, Mackiewicz J and Rutkowski P. First-line treatment of advanced/metastatic melanoma with anti-PD-1 antibodies: multicenter experience in Poland. Immunotherapy 2021; 13: 297-307.

[44] Lobefaro R, Viscardi G, Di Liello R, Massa G, Iacovino ML, Sparano F, Della Corte CM, Ferrara R, Signorelli D, Proto C, Prelaj A, Galli G, De Toma A, Brambilla M, Ganzinelli M, Trevisan B, Ciardiello F, De Braud F, Morgillo F, Garassino MC and Lo Russo G. Immunotherapy in advanced non-small cell lung cancer patients with poor performance status: the role of clinical-pathological variables and inflammatory biomarkers. Lung Cancer 2021; 152: 165-173.

[45] Facchinetti F, Di Maio M, Perrone F and Tiseo M. First-line immunotherapy in non-small cell lung cancer patients with poor performance status: a systematic review and meta-analysis. Transl Lung Cancer Res 2021; 10: 2917-2936.

[46] Cristescu R, Mogg R, Ayers M, Albright A, Murphy E, Yearley J, Sher X, Liu XQ, Lu H, Nebozhyn M, Zhang C, Lunceford JK, Joe A, Cheng J, Webber AL, Ibrahim N, Plimack ER, Ott PA, Seiwert TY, Ribas A, McClanahan TK, Tomassini JE, Loboda A and Kaufman D. Pan-tumor genomic biomarkers for PD-1 checkpoint blockade-based immunotherapy. Science 2018; 362: eaar3593.